Hindawi Publishing Corporation
EURASIP Journal on Advances in Signal Processing
Volume 2007, Article ID 42472, 10 pages
doi:10.1155/2007/42472

Research Article

Locally Adaptive DCT Filtering for Signal-Dependent Noise Removal

Ruşen Öktem,[1] Karen Egiazarian,[2] Vladimir V. Lukin,[3] Nikolay N. Ponomarenko,[3] and Oleg V. Tsymbal[4]

[1] *Electrical and Electronics Engineering Department, Atılım University, Kızılcaşar Köyü, 06836 İncek, Ankara, Turkey*
[2] *Institute of Signal Processing, Tampere University of Technology, 33101 Tampere, Finland*
[3] *Department of Receivers, Transmitters and Signal Processing, National Aerospace University, 17 Chkalova Street, 61070 Kharkov, Ukraine*
[4] *Kalmykov Center for Radiophysical Sensing of Earth, 12 Ak. Proskury Street, 61085 Kharkov, Ukraine*

Received 13 October 2006; Revised 21 March 2007; Accepted 13 May 2007

Recommended by Stephen Marshall

This work addresses the problem of signal-dependent noise removal in images. An adaptive nonlinear filtering approach in the orthogonal transform domain is proposed and analyzed for several typical noise environments in the DCT domain. Being applied locally, that is, within a window of small support, DCT is expected to approximate the Karhunen-Loeve decorrelating transform, which enables effective suppression of noise components. The detail preservation ability of the filter allowing not to destroy any useful content in images is especially emphasized and considered. A local adaptive DCT filtering for the two cases, when signal-dependent noise can be and cannot be mapped into additive uncorrelated noise with homomorphic transform, is formulated. Although the main issue is signal-dependent and pure multiplicative noise, the proposed filtering approach is also found to be competing with the state-of-the-art methods on pure additive noise corrupted images.

1. INTRODUCTION

Digital images are often degraded by noise, due to the imperfection of the acquisition system or the conditions during the acquisition. Noise decreases the perceptual quality by masking significant information, and also degrades performance of any processing applied over the acquired image. Hence, image prefiltering is a common operation used in order to improve analysis and interpretation of remote sensing, broadcast transmission, optical scanning, and other vision data [1, 2].

Till now a great number of different image filtering techniques have been designed including nonlinear nonadaptive and adaptive filters [3, 4], transform-based methods [5–11], techniques based on independent component analysis (ICA), and principal component analysis (PCA) [12, 13], and so forth. These techniques have different advantages and drawbacks thoroughly discussed in [3, 4, 14], and other references. The application areas and conditions for which the use of these filters can be the most beneficial and expedient depend on the filter properties, noise statistical characteristics, and the priority of requirements. For effective filtering, it is desirable to considerably suppress noise in homogeneous (smooth) regions and to preserve edges, details, and texture at the same time. Acceptable computational cost is the most important requirement that can restrict a practical applicability of some denoising techniques, for example, those based on ICA and PCA [12–14].

From the viewpoint of noise suppression, preservation of edges, details and texture, and time efficiency requirements, quite good effectiveness has been demonstrated by locally adaptive methods [15–17]. The latest modifications of locally adaptive filters [16, 17] include both typical nonlinear scanning window filters (employing order statistics) and transform-based filters, in particular, filters based on discrete cosine transform (DCT).

For many image denoising applications, it is commonly assumed that the dominant noise is additive and its probability density function (*pdf*) is Gaussian [3, 4, 18]. For microwave radar imagery, however, multiplicative noise is typical. The *pdf* of the noise can be either considered Gaussian or non-Gaussian (e.g., Rayleigh, negative exponential, gamma) depending on the radar type and its characteristics [15, 16, 19]. Images scanned from photographic or some

medical images are other examples [6] where additive Gaussian noise model fails.

Homomorphic transformation can sometimes be a reasonable way of converting signal-dependent or pure multiplicative noise to an additive noise, which then can be filtered appropriately [4, 16, 20–22]. However, quite often achievable benefits are not so obvious [21, 22] and without losing efficiency, it is possible to perform filtering without applying a homomorphic transformation to data (e.g., film-grain noise). Lee or Kuan filters [23, 24] are among those conventional and widely used techniques that aim to suppress multiplicative noise without the use of the homomorphic transform. The performance of such filters is improved by their integration into an iterative approach [25, 26]. However, iterative techniques are usually computationally costly, and they often may introduce oversmoothing.

In this work, we aim to develop a class of transform-based adaptive filters capable of suppressing signal-dependent and multiplicative noise, while preserving *texture, edges, and details*, which contain significant information for further processing and interpreting of images. In Section 2, we briefly overview a nonlinear transform domain filtering (how it is derived from a least mean square sense optimal filtering), for additive Gaussian noise. Note that any decorrelating orthogonal transform will be a possible choice for a transform domain filtering approach. Yet, we concentrate on the DCT in the following sections, discussing why we expect it to be a good choice for the transform domain filtering. In Section 3, we propose our local adaptive DCT (LADCT) filter in the presence of signal-dependent and multiplicative noise. For signal-dependent and multiplicative noise, we treat two cases separately: where the homomorphic transform can be and cannot be applied.

2. A BRIEF OVERVIEW OF TRANSFORM DOMAIN FILTERS FOR ADDITIVE GAUSSIAN NOISE

A general observation model for noise (we deal within this paper) can be expressed as

$$g_{ij} = f_{ij} + f_{ij}^{\gamma} \cdot n_{ij}, \tag{1}$$

where g_{ij}, f_{ij}, and n_{ij} denote the noisy image sample (pixel) value, true image value, and signal-independent noise component that is characterized by the variance σ_n^2, respectively, for the ijth sample. This model is a quite universal one, covering pure additive, signal-dependent, and pure multiplicative noise cases. Let

$$\hat{\mathbf{f}} = \mathbf{H} \cdot \mathbf{g} \tag{2}$$

denote a linear filtering operation, where $\hat{\mathbf{f}}$ and $\mathbf{g}$ refer to the vector of estimated signal and the observed (noisy) signal, respectively, and $\mathbf{H}$ refers to the matrix of linear filter coefficients.

Consider the case where $\gamma = 0$, corresponding to corruption with additive zero mean Gaussian noise (which is a valid assumption for many practical applications [3, 4, 18]). The coefficients of the linear optimal filter in the minimum mean square error sense for this case is the one which minimizes the mean square error between $\hat{\mathbf{f}}$ and $\mathbf{f}$, and will be denoted as

$$\mathbf{H} = \mathbf{R}_{ff}\left(\mathbf{R}_{ff} + \sigma_n^2\mathbf{I}\right)^{-1}. \tag{3}$$

In (3), $\mathbf{R}_{ff}$ is the correlation matrix of original data vector, $\mathbf{f}$. Let $\mathbf{U}$ and Δ be the matrices with eigenvectors and eigenvalues of $\mathbf{R}_{ff}$, respectively, that is, $\mathbf{R}_{ff} = \mathbf{U}\Delta\mathbf{U}^T$. Then the filtering matrix (3) becomes

$$\mathbf{H} = \mathbf{U}(\mathbf{I} + \sigma_{\mathbf{n}}^2\Delta^{-1})\mathbf{U}^T = \mathbf{U}\widetilde{\Delta}\mathbf{U}^T, \tag{4}$$

where $\widetilde{\Delta} = \mathrm{diag}\{\lambda_1/(\lambda_1+\sigma_n^2), \lambda_2/(\lambda_2+\sigma_n^2), \ldots, \lambda_M/(\lambda_M+\sigma_n^2)\}$, λ_i being the eigenvalues of $\mathbf{R}_{ff}$. Equation (4) can be interpreted as mapping the signal into the Karhunen-Loeve transform (KLT) domain, processing each coefficient individually, and then mapping the processed coefficients back to the time/space domain.

Recall that in practical signal processing applications, due to the need for a priori knowledge of the original signal statistics, KLT is often replaced by a decorrelating transform with fixed basis functions such as discrete cosine transform (DCT) [27] or discrete wavelet transform (DWT) [8–11, 28, 29]. Energy compaction and decorrelation are two important properties of orthogonal transforms exploited in denoising applications [5], because energy of white Gaussian noise is uniformly diffused over all vectors of any orthogonal transform, and it is desirable to find a basis, which has appropriately good energy compaction property for a near-optimum denoising.

DWT methods are generally the extensions to the work of Donoho and Johnstone [30], where $\mathbf{U}$ is replaced with $\mathbf{U}_a$, representing DWT, and $\widetilde{\Delta}$ is approximated with $\Delta_{\mathbf{a}} = \mathrm{diag}\{\lambda_1^a, \lambda_2^a, \ldots, \lambda_M^a\}$, where

$$\lambda_i^a = \begin{cases} 1, & \left|\left(\mathbf{U}_a^T\mathbf{g}\right)_i\right| > \mathrm{thr} \\ 0, & \text{else,} \end{cases} \tag{5}$$

or

$$\lambda_i^a = \begin{cases} \mathrm{sgn}\left[\left(\mathbf{U}_a^T\mathbf{g}\right)_i\right] \cdot \left|\left(\mathbf{U}_a^T\mathbf{g}\right)_i - \mathrm{thr}\right|, & \left|\left(\mathbf{U}_a^T\mathbf{g}\right)_i\right| > \mathrm{thr} \\ 0, & \text{else,} \end{cases} \tag{6}$$

and $(\mathbf{U}_a^T\mathbf{g})_i$ corresponds to the ith sample of the vector $\mathbf{U}_a^T\mathbf{g}$. The expression in (5) is referred to as a hard thresholding and the one in (6) is a soft thresholding, thr denoting a preset threshold. Donoho and Johnstone have proven that both schemes are within the logarithmic factor of the mean square error, and proposed $\mathrm{thr} = k \cdot \sigma_n$, where $k = 2\sqrt{\ln M}$ (M denoting the length of the signal).

In DCT-based denoising, block-based processing is often preferred [27], since this not only enables fast and memory efficient implementations but also exploits local quasi-stationary behavior of images. DCT approximates KLT for highly correlated data in a windowed region of natural images [31]. Two other clear advantages of DCT are that, being

involved in standard compression schemes [32], fast implementation structures have been widely developed and DCT-based implementations can easily be embedded in those standard schemes.

3. DCT FILTERING FOR MULTIPLICATIVE AND SIGNAL-DEPENDENT NOISE CASES

As it was mentioned earlier, multiplicative noise is typical for radar and ultrasound imaging systems [15, 19, 20]. The noise characteristics in radar images depend upon several factors such as a system type—whether one deals with an image obtained by synthetic aperture radar (SAR) or side look aperture radar (SLAR) [15, 19]. Additionally, multiplicative noise (speckle) characteristics are determined by a radar operation mode, for example, is a SAR image one look or multilook. The simplified radar image models commonly take the multiplicative noise into account only, and can be described by (1), when $\gamma = 1$ [19]. Then, (1) can be updated as follows:

$$g_{ij} = f_{ij} + f_{ij} \cdot n_{ij} = f_{ij}\mu_{ij}, \tag{7}$$

where the multiplicative noise factor can also be expressed as $\mu_{ij} = 1 + n_{ij}$. According to (1), the variance σ_μ^2 of the variable μ is similar to σ_n^2 for $\gamma = 1$. Note that σ_μ^2 is often referred to as multiplicative noise or speckle (relative) variance.

In SLAR image case, μ is Gaussian with its mean value equal to unity. For the simplified model (7) of a pure multiplicative noise, the influence of a radar point spread function and an additive noise is often neglected. In most of the real cases σ_μ^2 is considered to be a constant value for the entire image. Typical values of σ_μ^2 are commonly of the order $0.004 \cdots 0.02$ for SLAR images and slightly larger for multilook SAR images [15, 33].

In SAR images, σ_μ^2 is determined by a method of forming a one-look SAR image and a number of looks N_{looks} used. Statistical experiments carried out using the standard χ^2 test show that if a one-look SAR image is formed as an estimate of the backscattered signal amplitude, then it is enough to have $N_{\text{looks}} > 8 \cdots 9$ in order to consider multiplicative noise Gaussian in obtained multilook SAR image. Similarly, if a one-look SAR image is formed as an estimate of the backscattered signal intensity (and *pdf* of original speckle in one-look SAR image is negative exponential), then $N_{\text{looks}} > 30 \cdots 35$ is enough to accept hypothesis on Gaussian *pdf* of multiplicative noise in multilook SAR image with a probability over 0.5. In other words, if in a multilook SAR image one has $\sigma_\mu^2 < 0.035$, an assumption on Gaussianity of multiplicative noise is valid.

As it is demonstrated in [15], the model (7) is, in general, applicable to describe radar images corrupted by nonsymmetric *pdf* speckle which is typical for images formed by SAR with a small number of looks [19]. Note that often the quality of original images and their filtered versions is expressed in terms of equivalent number of looks [19]. It is also worth noting that if the corresponding prefiltering of images with non-Gaussian speckle has been carried out, the residual noise in homogeneous regions, being still multiplicative, approximately obeys Gaussian distribution [15, 33].

It directly follows from (1) and (7) that, in the homogeneous regions of SLAR and SAR images, local variance $\sigma_{\overline{g}}^2$ of fluctuations due to multiplicative noise (speckle) is strictly connected with the local mean $\overline{g}_{\text{loc}}$: $\sigma_{\overline{g}}^2 \approx \sigma_\mu^2 \overline{g}_{\text{loc}}^2$ [15, 19]. This property is widely exploited in denoising of images corrupted by multiplicative noise [23–26].

3.1. *Local adaptive filtering for pure multiplicative noise* ($\gamma = 1$)

In order for us to cope with the multiplicative noise, nonlinear transform domain denoising described in Section 2 can be combined with the homomorphic transformation [15, 22] that converts the multiplicative noise into additive noise. Note that the use of the homomorphic transformations is a commonly recommended way for processing of data corrupted by a multiplicative noise [4]. Its basic motivation is that this leads to reduced complexity (simplification) of situation one has to deal with. This is true in some cases, but not always.

In this case, we obtain a denoising scheme where the input passes through the homomorphic transformation of the logarithmic type at first, then a denoising operation is performed, and finally, the obtained image is subject to the inverse homomorphic transformation. Such scheme can be denoted as Hom $\rightarrow H \rightarrow$ Hom^{-1} where Hom and Hom^{-1} denote a pair of direct and inverse homomorphic transforms, respectively, and H denotes the applied filter.

Note that after Hom, one can obtain additive noise with probability density function close to Gaussian if and only if: originally pure multiplicative noise has been Gaussian and this noise has been characterized by a rather small relative variance σ_μ^2 (the tests have shown that it should be smaller than 0.02). In all other cases, the obtained additive noise does not obey Gaussian distribution and this can cause problems in transform-based denoising. For example, this happens for images corrupted by nonsymmetric pdf speckle (Rayleigh, negative exponential, gamma, etc.) that are typical for images formed by SARs with one or few looks [15, 20, 22]. After direct homomorphic transform of logarithmic type such speckle noise becomes additive but also nonsymmetric (with respect to its mean) and heavy tailed. Removal of such noise is not a typical and simple task. In other words, the situation after transformation does not become simpler than it was before it.

In [16], it was proposed to convert a multiplicative noise as expressed by (7) to an additive noise by means of the direct homomorphic transform $g_{ij}^h = [a \log_b(g_{ij})]$, where a and b are constants and $[\cdot]$ denotes rounding-off to the nearest integer. The recommended values of a and b for the traditional 8-bit representation of gray-scale images were equal to 8.39 and 1.2, respectively. If $\sigma_\mu^2 \leq 0.02$, for the images obtained after aforementioned direct homomorphic transform, noise could be considered Gaussian, additive with zero mean and variance equal to $\sigma_{\text{additive}}^2 = a^2 \cdot \sigma_\mu^2/(\ln b)^2$.

On one hand, according to our investigations [16], rounding-off to the nearest integer introduces some distortions (additional errors) due to direct and, then, inverse

homomorphic transforms, that is, g_{ij} can be only approximately equal to $\mathrm{Hom}^{-1}(\mathrm{Hom}(g_{ij}))$. In general, filtering can be applied to data represented as floating point values. On the other hand, the application of DCT and other transform-based filters to integer-valued data commonly provides considerably better computational efficiency than if these filters are applied to real valued images [34].

Therefore, the image processing scheme Hom $\rightarrow$ H $\rightarrow$ Hom^{-1} has some restrictions in terms of its application in practice. At the same time, in the case of pure multiplicative noise there is another possibility to perform a local DCT-based filtering. For this purpose, we prefer to approximate the filtering operation of (4) in the DCT domain by exploiting the thresholding operation in (5)-(6) with an adaptive scheme. Note that when the denoised image pixels in each block are obtained directly through the inverse DCT of the thresholded coefficients for that block as in [27], pseudo-Gibbs phenomena, that is, undershoots and overshoots, around the neighborhood of discontinuities occur [28]. In order to overcome this, we propose to generate multiple denoised estimates instead of a single one, for each pixel in the block at first. Then, the filtered intensity value for a particular pixel can be obtained through averaging (weighted averaging) over those multiple estimates. Neighboring and overlapping blocks can provide multiple estimates, when the block window is sliding in the vertical and horizontal directions. Averaging over multiple estimates suppresses undershoots and overshoots, in a way analogous to the translation invariant denoising proposed by Coifman and Donoho in [28]. The main idea is to decrease the effect of misalignment between the signal and the basis function, by shifting the signal a number of times.

This *algorithm* of DCT-based denoising can be, in general, summarized below.

(1) Divide an image to be processed into overlapping blocks (scanning windows) of size $M \times M$; let s be a shift (in one dimension, row, or columnwise) in pixels between two neighboring overlapping blocks.

(2) For each block, with the left upper corner in the ijth pixel, assign

$$x(m,l) = g(i+m, j+l), \quad m,l = 0,\ldots,M-1. \tag{8}$$

(i) Calculate the DCT coefficients as follows:

$$\begin{aligned} X[p,q] =& c[p]c[q] \sum_{m=0}^{M-1}\sum_{l=0}^{M-1} x(m,l) \\ &\times \cos\left[\frac{(2m+1)p\pi}{2M}\right]\cos\left[\frac{(2l+1)q\pi}{2M}\right], \end{aligned} \tag{9}$$

where

$$c[p] = \begin{cases} \sqrt{\dfrac{2}{M}}, & 1 \le p \le M-1, \\ \dfrac{1}{\sqrt{M}}, & p = 0, \end{cases}$$

$$c[q] = \begin{cases} \sqrt{\dfrac{2}{M}}, & 1 \le q \le M-1, \\ \dfrac{1}{\sqrt{M}}, & q = 0. \end{cases} \tag{10}$$

(ii) Apply thresholding to the DCT coefficients $X[p,q]$ according to the selected type of thresholding (either hard (5) or soft (6)) and obtain $X_{\mathrm{th}}[p,q]$.

(iii) Obtain the estimates within each block by applying the inverse DCT to the thresholded transform coefficients as

$$\begin{aligned} x_f(m,l) =& c[p]c[q] \sum_{p=0}^{M-1}\sum_{q=0}^{M-1} X_{\mathrm{th}}[p,q] \\ &\times \cos\left[\frac{(2m+1)p\pi}{2M}\right]\cos\left[\frac{(2l+1)q\pi}{2M}\right]. \end{aligned} \tag{11}$$

(iv) Get the filtered values for the block as

$$\hat{f}(i+m, j+l) = x_f(m,l), \quad m,l = 0,\ldots,M-1. \tag{12}$$

(3) Obtain the final estimate $\hat{f}_{ij}^{f}$ for a pixel at ijth location by averaging the multiple estimates of it, these come from neighboring overlapping blocks including that pixel.

If the homomorphic transform is not applied, there is the following distinction. For the thresholding step, (2)(ii), we propose to adjust the threshold value for each image block separately (individually). Specifically, a rough supposition can be made that a noise within a small image block is close to additive. In this case, the noise variance within the block can be calculated as $\sigma_g^2 \approx \overline{g}^2 \cdot \sigma_\mu^2$ where $(\overline{g})$ is the local mean of the pixels in this block. Thus, the threshold value for each block should be chosen as $k \cdot \sigma_\mu \cdot \overline{g}$ where k is a constant (more thorough background is given in the next subsection). We refer to this algorithm for denoising of multiplicative noise as local adaptive DCT denoising with s number of overlaps (LADCT-s). The same algorithm when fixed threshold is used is referred to as LDCT throughout the paper.

If one uses a scheme Hom $\rightarrow$ H $\rightarrow$ Hom^{-1} where H is the DCT-based filtering *algorithm* described above, Hom should be applied to the whole image before step 1, with obtaining $g_{ij}^{h} = [a \log_b(g_{ij})]$ and applying all steps 1–3 to g^h. As the result, after executing step 3, one obtains $\hat{f}_h^f$ and then for an entire image, the inverse homomorphic transform will be performed to obtain the filtered image $\hat{f}^f$. In that case, a threshold value used at the step (2)(ii) will be fixed for all blocks used, $\mathrm{thr} = k \cdot \sigma_{\mathrm{additive}}$ with $\sigma_{\mathrm{additive}} = a \cdot \sigma_\mu/(\ln b)$. Similarly, one has to set $\mathrm{thr} = k \cdot \sigma_n$ if a noise is pure additive ($\gamma = 0$ in the model (1)).

Although we study a multiplicative noise model in this work, we compared the performance of the above proposed algorithm in presence of additive Gaussian noise with that of the state-of-the-art wavelet denoising methods [8, 9, 11, 29]. Our simulations showed that the proposed algorithm competes with GSMWD, which is reportedly one of the best denoising methods in the literature. Gaussian scale mixtures

Table 1: PSNR results of processing the test image including texture regions, corrupted by multiplicative noise, $\sigma_\mu^2 = 0.012$.

Denoising techniques	Thresholding type and threshold value	Local PSNR, dB
Original image	—	23.62
Haar wavelet	Soft: $1.2\sigma_n$	26.39
Haar wavelet	Hard: $2.8\sigma_n$	27.63
Symmlet wavelet	Soft: $1.2\sigma_n$	27.37
Symmlet wavelet	Hard: $2.6\sigma_n$	27.96
Extended symmlet wavelet	Soft, auto-adjusting of threshold	28.26
LDCT-1	Hard: $2.6\sigma_n$	**28.76**
LADCT-1	Hard with adaptation: $k = 2.6$	**28.91**

in the wavelet domain (GSMWD) [29] is a wavelet denoising technique based on a local Gaussian scale mixture model in an overcomplete oriented pyramid representation. The performance of DCT-based denoising for additive Gaussian noise can be increased with weighted processing of estimates obtained from different overlapping blocks like in [35, 36] or by the use several transforms in a switch [36], of nonequal shape and size of blocks (http://www.cs.tut.fi/~foi/SA-DCT), and so forth.

3.2. Experimental results with pure multiplicative noise ($\gamma = 1$)

Let us now analyze and compare the performance of the scheme Hom $\rightarrow H \rightarrow$ Hom^{-1}, the proposed LADCT-s, and some other filters. First, we consider a particular task of texture preservation. In [16], we have thoroughly discussed texture preserving properties of a wide set of different filters. It has been demonstrated that the procedure Hom $\rightarrow H \rightarrow$ Hom^{-1} where H was DCT-based filtering for additive noise outperformed such good detail preserving filters like standard and modified sigma filters [33], local statistic Lee [23], FIR median hybrid and center weighted median filters [3], and so forth. However, the comparison to wavelet-based denoising methods has not been carried out.

The studies in [16] have been accomplished for the cases of prevailing Gaussian multiplicative noise with relative variance values $\sigma_\mu^2 = 0.005$ and $\sigma_\mu^2 = 0.012$ typical for SLAR images. These values satisfy aforementioned condition $\sigma_\mu^2 \leq 0.02$. Below we consider a particular case of $\sigma_\mu^2 = 0.012$.

Taking into account the fact that wavelet-based denoising is commonly applied to images corrupted by additive noise, let us perform a performance comparison between wavelet and DCT-based denoising methods under an assumption of transform-based filter to be used within the scheme Hom $\rightarrow H \rightarrow$ Hom^{-1}, that is, in fact, for additive noise. For this purpose, let us consider the same test image as that one used in [16] (see Figure 1). Among the wavelet denoising techniques the following have been examined: the Haar wavelet, the Daubechies, and Symmlet wavelets, all with hard (HT) and soft (ST) thresholding. The obtained data are presented in Table 1. Note that DCT-based filtering with hard thresholding (thr $= 2.6\sigma_n$) and $s = 1$ has been used. We have also tested the proposed LADCT-s (the last row in Table 1) directly on noisy image (without homomorphic transforms). The listed threshold values in Table 1 are the ones for which corresponding wavelet denoising techniques provide the best local PSNR for texture regions and near best PSNR for the entire image. Local PSNR has been computed as $\text{PSNR}_{\text{loc}} = 10 \cdot \log(255^2/\text{MSE}_{\text{loc}})$ where MSE_{loc} has been calculated for all pixels belonging to all four texture regions in the test image (see Figure 1). All wavelet denosing techniques have been implemented by the software tool obtained from WaveLab for MATLAB (www-stat.Stanford.edu).

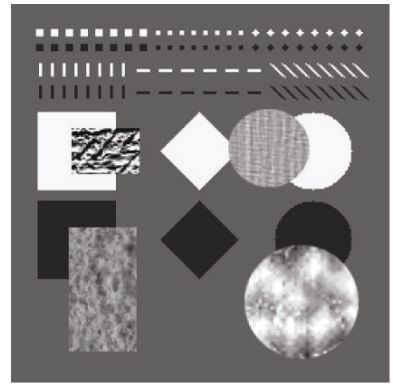

Figure 1: The noise-free test image with four texture regions (two of rectangular and two of circular shape).

As seen, for textural regions both DCT-based filtering techniques produce the best (largest) local PSNRs. They are by $0.5 \cdots 2.5$ dB better than for the considered wavelet denosing schemes. The scheme Hom $\rightarrow$ LDCT-1 $\rightarrow$ Hom^{-1} and LADCT-1 produce practically equal PSNR_{loc} although for the latter technique PSNR_{loc} is slightly larger. Since LADCT-1 does not require performing homomorphic transformations and the only additional operations are calculation of local means in all blocks and their multiplying by $k\sigma_\mu$ (both are very simple), practical application of LADCT-1 seems preferable in comparison to Hom $\rightarrow$ LDCT-1 $\rightarrow$ Hom^{-1}.

This conclusion has also been confirmed by simulation data presented in our earlier paper [22]. It is shown there for the test image "Montage" corrupted by pure multiplicative noise with $\sigma_\mu^2 = 0.035$ that PSNR values for LADCT-1 are

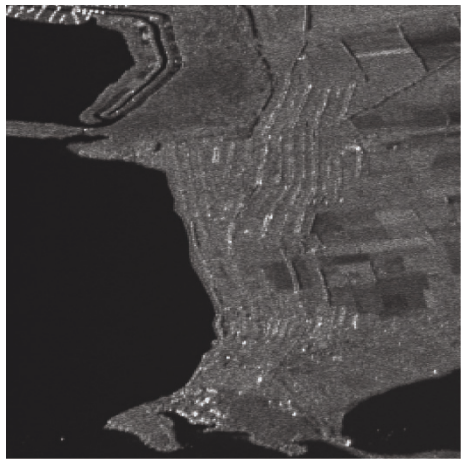

(a)

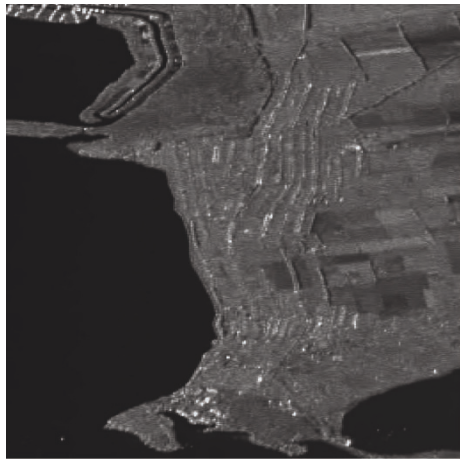

(b)

Figure 2: Original SLAR image (a) and the output image after applying LADCT-1 (b).

Table 2: PSNR results for Boat, degraded with multiplicative noise, $\gamma = 1$.

σ_μ	Kuan[1] [25]	Kuan[3] [25]	LADCT-1
0.1	29.72	30.88	32.24
0.2	25.74	26.81	28.88
0.3	22.85	23.65	26.84

about 0.6 dB better than for the scheme Hom → LDCT-1 → Hom^{-1}.

An example of applying LADCT-1 with hard thresholding ($k = 2.6$) to a real SLAR image with $\sigma_\mu^2 = 0.012$ is presented in Figure 2(a). Noise is well seen, especially in image regions with rather large local mean. The obtained output image is shown in Figure 2(b). Noise is considerably suppressed in image homogeneous regions while useful information like edges, fine details, and texture is preserved well.

Table 3: SNR results for Lenna, degraded with 16-looks speckle noise.

Noisy image	Kuan	FMP [37]	LADCT-1
7.8 dB	16.1	19.1 dB	19.8 dB

We also have compared our method LADCT-1 (hard thresholding, $k = 2.6$) with the one of the most recent and competitive method called fuzzy matching pursuit (FMP) [37]. Recursive Kuan filters [25] and conventional Kuan filters [24] have been also considered. The results are presented in Tables 2, 3. They show the superiority of local adaptive DCT filtering (LADCT) for removing pure multiplicative noise. LADCT-1 outperforms Kuan filter-based iterative technique by approximately 2 dB (see data in Table 2) and the FMP based technique by 0.7 dB (see data in Table 3). Note that advantages of LADCT (larger PSNR or SNR values) become especially obvious for more intensive multiplicative noise (large values of σ_μ).

One more example of using LADCT-1 with hard thresholding ($k = 2.6$) is given in Figure 3. An original image was formed by a two-look SLAR image where each look image represent a spatial estimate of reflected signal amplitude. Thus, σ_μ^2 is about 0.14. As expected, speckle is well seen visually and it is rather intensive. The output image is demonstrated in Figure 3(b). Fine details and edges are perfectly retained while in image homogeneous regions noise is suppressed well.

Above we prefer to use SNR or PSNR as the quantitative measures of filtering performance. Sometimes, equivalent number of looks is employed to characterize and compare the performance of different filters. But this criterion basically relates to noise suppression in image homogeneous regions while integral and local PSNR values are able to quantitatively describe filter effectiveness for entire images and their fragments, respectively.

3.3. *Local adaptive filtering for film-grain noise* ($0 < \gamma < 1$)

The type of noise described by (1) when $0 < \gamma < 1$ is generally referred as film-grain noise, and occurs when photographic films are scanned, due to the granularity of photo-sensitive crystals on the film [24, 26]. It is a special case where it is not possible to reform (1) into (7) *by homomorphic transforms*. Most of the existing methods for removing such type of noise rely on recursive filtering [25, 26]. In [6], an approximation of mean square error filtering in the transform domain is formulated, and a wavelet domain denoising method is proposed as a faster and edge preserving filtering alternative to recursive type of filters. Here, we revisit the mean square error filtering approach, and propose a DCT domain filter, which exploits local stationary characteristics of natural images.

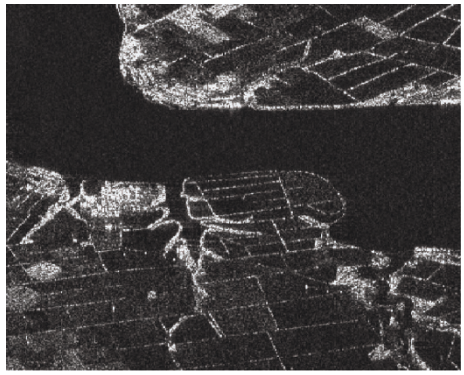

(a)

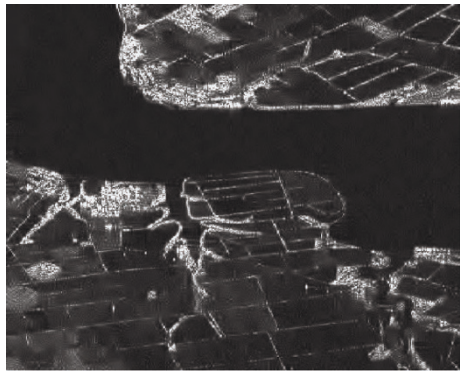

(b)

Figure 3: Original SAR image (a) and the output image after applying LADCT-1 (b).

Let us get back to the filtering operation expressed by (2), where the noisy image is expressed as in (1). Then the optimum filter H_γ, in the least mean square error sense will be

$$\mathbf{H}_\gamma = \mathbf{R}_{ff}\left(\mathbf{R}_{ff} + \sigma_n^2\mathbf{R}_\gamma\right)^{-1}, \tag{13}$$

where $\mathbf{R}_\gamma$ stands for the autocorrelation matrix $\mathbf{f}_\gamma = [f_1^\gamma, f_2^\gamma, \ldots, f_M^\gamma]^T$, f_i representing the original data samples. Equation (13) can be reformulated as

$$\mathbf{H}_\gamma = \mathbf{U}\left(\mathbf{I} + \sigma_n^2\mathbf{U}^T\mathbf{R}_\gamma\mathbf{U}\boldsymbol{\Delta}^{-1}\right)^{-1}\mathbf{U}^T = \mathbf{U}\left(\mathbf{I} + \sigma_n^2\widetilde{\mathbf{R}}_\gamma\boldsymbol{\Delta}^{-1}\right)^{-1}\mathbf{U}^T, \tag{14}$$

where $\mathbf{R}_{ff} = \mathbf{U}\boldsymbol{\Delta}\mathbf{U}^T$ and $\widetilde{\mathbf{R}}_\gamma = \mathbf{U}^T\mathbf{R}_\gamma\mathbf{U}$. Consider the case of slowly varying data, such as f_i varies in close vicinity of its mean $\overline{f}$. That is, the data vector can be expressed as

$$\mathbf{f} = \left[\overline{f} + \delta_1, \overline{f} + \delta_2, \ldots, \overline{f} + \delta_M\right]^T, \tag{15}$$

where δ_i are zero mean iid random variables with variance σ_δ^2. When σ_δ^2 is small enough, then, the γth root of f_i can be approximated as $\mathbf{f}_\gamma = [\overline{f}^\gamma + \delta_1', \overline{f}^\gamma + \delta_2', \ldots, \overline{f}^\gamma + \delta_M']^T$, where δ_i' are zero mean iid random variables with variance $\sigma_{\delta'}^2 \le \sigma_\delta^2$. In that case, the autocorrelation matrices $\mathbf{R}_{ff}$ and $\mathbf{R}_\gamma$ can be expressed as $\mathbf{R}_{ff} = \overline{f}^2 \cdot \mathbf{P} + \sigma_\delta^2 \cdot \mathbf{I}$, $\mathbf{R}_\gamma = \overline{f}^{2\gamma} \cdot \mathbf{P} + \sigma_{\delta'}^2 \cdot \mathbf{I}$ where $\mathbf{P}$ refers to the matrix of ones. Then, the matrix which diagonalizes $\mathbf{R}_{ff}$ also diagonalizes $\mathbf{R}_\gamma$, and (14) reduces to the same form as (4),

$$\mathbf{H}_\gamma = \mathbf{U}\widetilde{\Delta}_\gamma\mathbf{U}^T, \tag{16}$$

where $\widetilde{\boldsymbol{\Delta}} = \operatorname{diag}\{\lambda_1/(\lambda_1 + \sigma_n^2 \cdot \overline{f}^{2\gamma}), \lambda_2/(\lambda_2 + \sigma_n^2 \cdot \overline{f}^{2\gamma}), \ldots, \lambda_M/(\lambda_M + \sigma_n^2 \cdot \overline{f}^{2\gamma})\}$, when $\sigma_{\delta'}^2$, σ_δ^2 terms are ignored. Our simulations show that the above statements related to $\mathbf{R}_{ff}$ and $\mathbf{R}_\gamma$ are accurate as long as (15) holds for $3 \cdot \sigma_\delta < \overline{f}$, which is a safe assumption within a small support of image data. Hence, the proposed algorithm in Section 3.1 can be used as an approximation to the filtering expressed by (16), when

$$\text{thr} = k \cdot \sigma_n \cdot \overline{f}^\gamma. \tag{17}$$

$\overline{f}$ denotes an approximation to the true data at the corresponding pixel, and we use the DC coefficient of the corresponding DCT block for it. Since the DC coefficient corresponds to sum of the pixel values in that block, scaled by $c[0]$ (see (9)), we further multiply it by $c[0]$ to obtain the sample mean of the block.

It follows from (17) that for a pure multiplicative noise ($\gamma = 1$) the threshold in each block is to be set as $k \cdot \sigma_\mu \cdot \overline{g}$, that is, our earlier intuitive assumption has been confirmed.

3.4. Experimental results with film-grain noise ($0 < \gamma < 1$)

We tested our formulation on Lenna, Barbara, and Boat images, for which either PSNR or SNR results with recent filtering techniques are available in the literature. Although k is recommended to be $2\sqrt{\ln M}$ ($= 2.9$ for $M = 8 \times 8$ window size) in [30], we performed and reported our simulations for $k = 2.6$ (which achieved better performance in our simulations), and used soft thresholding. The corrupted images are generated by using the film-grain noise model with $\gamma = \{0.2, 0.4, 0.6\}$. We have compared our results with AWD [6] and multiscale local linear minimum mean square error filter (LLMMSE) [38]—an improvement of the Kuan filter. AWD is a wavelet denoising technique developed for data-dependent noise removal, which uses adaptive thresholding. The threshold is calculated by using previously filtered low resolution subband samples in a wavelet decomposition hierarchy.

The results for LADCT-1 are considerably better than those for LADCT-8 (compare data in two rightmost columns in Tables 4–6). LADCT-1 performs 1.4 dB to 2.1 dB better than multiscale LLMMSE filter for Lenna image (see Table 4). The results of multiscale LLMMSE filter do

Table 4: SNR results for Lenna, degraded with film-grain type of noise at 2.9 dB.

γ	LLMMSE	M-LLMMSE	AWD [6]	LADCT-8	LADCT-1
0.2	12.0	14.7	14.3	14.3	16.1
0.4	12.1	14.8	14.9	15.2	16.8
0.6	12.3	15.0	14.9	15.3	17.1

Table 5: SNR results for Boat, degraded with film-grain type of noise at 2.9 dB SNR.

γ	LLMMSE		AWD [6]		LADCT-8		LADCT-1	
	Overall	Detail	Overall	Detail	Overall	Detail	Overall	Detail
0.2	10.27	7.44	10.72	7.36	11.05	7.71	12.94	10.30
0.4	10.31	7.57	10.81	7.61	11.08	7.33	12.98	10.45
0.6	10.46	7.84	10.86	7.85	11.69	8.05	13.12	10.31

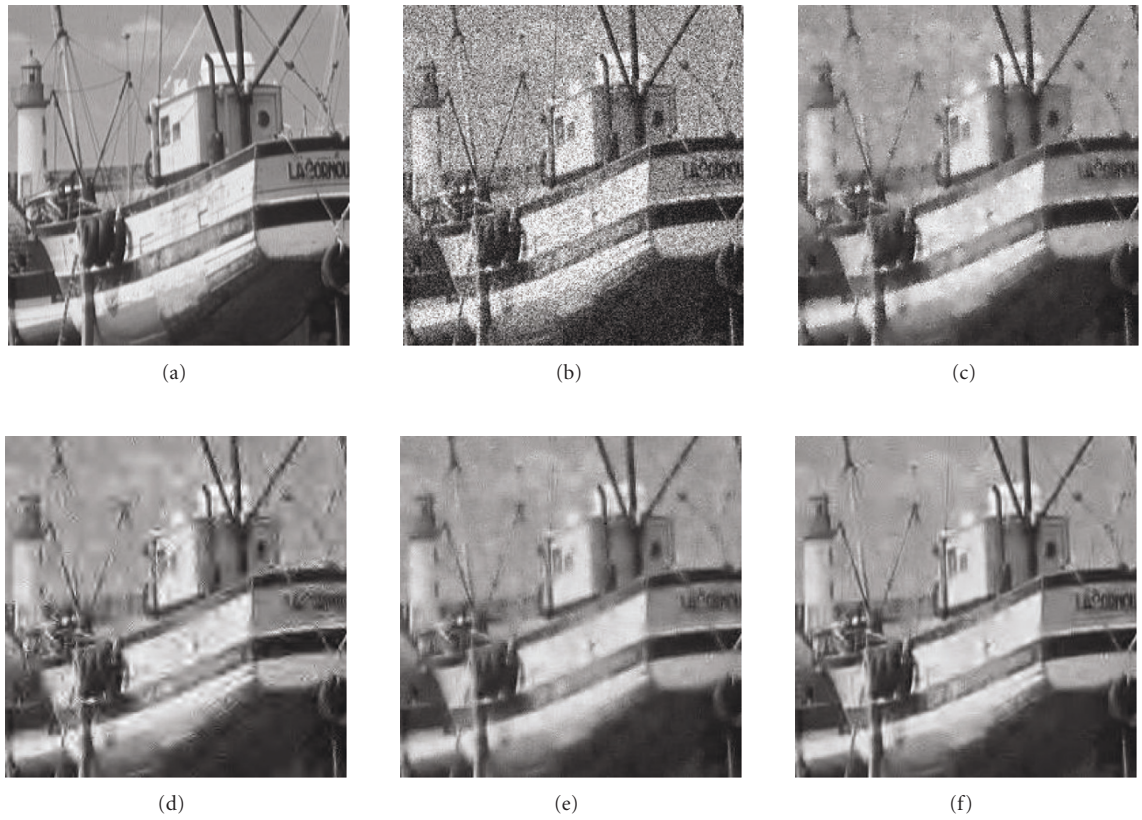

(a) (b) (c)

(d) (e) (f)

Figure 4: Portion of the Boat image: (a) original, (b) film-grain noised at 2.9 dB ($\gamma = 0.4$), (c) LLMMSE filtered, (d) adaptive wavelet denoised, (e) LADCT-8, (f) LADCT-1 filtered.

Table 6: SNR results for Barbara, degraded with film-grain type of noise at 2.9 dB SNR.

γ	LLMMSE	AWD [6]	LADCT-8	LADCT-1
0.2	9.66	9.89	10.49	12.60
0.4	9.67	9.83	10.46	12.90
0.6	9.67	9.78	10.51	12.62

not exist for Boat and Barbara test images in the literature. Compared to LLMMSE filter, LADCT-1 outperforms it by ∼4.5 dB, ∼2.6 dB, ∼3 dB for Lenna, Boat, and Barbara, respectively. Even when there is no overlapping of blocks (denoted as LADCT-8), LADCT slightly outperforms M-LLMMSE, and outperforms LLMMSE by from 0.8 to 3.1 dB. The SNR values obtained for LADCT-1 are also considerably better than for the AWD filter [6]. Note that in Table 5 we give not only SNR values calculated for entire (overall) test image, but also the values of local SNR determined for heterogeneous (detail) regions of the test image Boat. Both overall and local SNRs for LADCT-1 are considerably better compared to the corresponding data for LLMMSE and AWD (see Table 5).

Subjective evaluations also favor LADCT. Figure 4 displays portions of the original, noisy (at 2.9 dB, $\gamma = 0.4$), and filtered Boat images. Figures 4(e)-4(f) present more pleasant display than the other two methods (wavelet denoising with adaptive thresholding [6] in Figure 4(d), and LLMMSE in Figure 4(c)). Figure 4(c) shows that LLMMSE especially fails in removing noise at and around the edges. It shows that LADCT-1 not only suppresses noise, but also preserves the details better than the competing techniques.

4. CONCLUSIONS

This work considers and introduces a class of transform domain filters for enhancing signal-dependent and multiplicative noise corrupted images. We address the case both when multiplicative noise can be and cannot be turned into additive noise with homomorphic transform. We show that optimal linear filtering in the least mean square error sense for both cases can be approximated by an adaptive thresholding scheme in the orthogonal transform domain, and discuss that block-based DCT is a preferable choice as the transform. We exploit the local sliding window (block) approach, which improves the performance by decreasing overshooting and undershooting artifacts of thresholding. The test results prove that our local adaptive DCT (LADCT) filters not only outperform existing filters attacking signal-dependent and multiplicative noise, but also compete with the state-of-the-art additive Gaussian noise filtering techniques. It is also illustrated by Figures and Tables that LADCT filters preserve details and texture better while removing noise at those regions.

REFERENCES

[1] R. M. Haralick and L. G. Shapiro, *Computer and Robot Vision*, Addison-Wesley, Reading, Mass, USA, 1992.

[2] N. Pierdicca, R. Crapolicchio, P. Basili, P. Ciotti, G. d'Auria, and F. S. Marzano, "Classification of multifrequency radar polarimetric data: role and contribution of vectorial filters," in *Proceedings of International Geoscience and Remote Sensing Symposium (IGARSS '95)*, vol. 3, pp. 1915–1917, Firenze, Italy, July 1995.

[3] J. Astola and P. Kuosmanen, *Fundamentals of Nonlinear Digital Filtering*, CRC Press LLC, Boca Raton, Fla, USA, 1997.

[4] I. Pitas and A. N. Venetsanopoulos, *Nonlinear Digital Filters: Principles and Applications*, Kluwer Academic Publishers, Dordrecht, The Netherlands, 1990.

[5] G. Strang and T. Nguyen, *Wavelets and Filter Banks*, Wellesley Cambridge Press, Wellesley, Mass, USA, 1996.

[6] R. Öktem and K. Egiazarian, "Transform domain algorithm for reducing effect of film-grain noise in image compression," *Electronics Letters*, vol. 35, no. 21, pp. 1830–1831, 1999.

[7] D. L. Donoho, "De-noising by soft-thresholding," *IEEE Transactions on Information Theory*, vol. 41, no. 3, pp. 613–627, 1995.

[8] A. A. Bharath and J. Ng, "A steerable complex wavelet construction and its application to image denoising," *IEEE Transactions on Image Processing*, vol. 14, no. 7, pp. 948–959, 2005.

[9] M. S. Crouse, R. D. Nowak, and R. G. Baraniuk, "Wavelet-based statistical signal processing using hidden Markov models," *IEEE Transactions on Signal Processing*, vol. 46, no. 4, pp. 886–902, 1998.

[10] L. Şendur and I. W. Selesnick, "Bivariate shrinkage functions for wavelet-based denoising exploiting interscale dependency," *IEEE Transactions on Signal Processing*, vol. 50, no. 11, pp. 2744–2756, 2002.

[11] P.-L. Shui, "Image denoising algorithm via doubly local Wiener filtering with directional windows in wavelet domain," *IEEE Signal Processing Letters*, vol. 12, no. 10, pp. 681–684, 2005.

[12] A. Hyvarinen, P. Hoyer, and E. Oja, "Image denoising by sparse code shrinkage," in *Intelligent Signal Processing*, S. Haykin and B. Kosko, Eds., pp. 554–568, IEEE Press, New York, NY, USA, 2001.

[13] D. D. Muresan and T. W. Parks, "Adaptive principal components and image denoising," in *Proceedings of IEEE International Conference on Image Processing (ICIP '03)*, vol. 1, pp. 101–104, Barcelona, Spain, September 2003.

[14] M. C. Motwani, M. C. Gadiya, R. C. Motwani, and F. C. Harris, "Survey of image denoising techniques," in *Proceedings of Global Signal Processing Expo and Conference (GSPx '04)*, Santa Clara, Calif, USA, September 2004.

[15] V. Melnik, "Nonlinear locally adaptive techniques for image filtering and restoration in mixed noise environments," Thesis for the degree of Doctor of Technology, Tampere University of Technology, Tampere, Finland, 2000, http://www.atilim.edu.tr/~roktem/Research/interests.htm.

[16] O. V. Tsymbal, V. V. Lukin, N. N. Ponomarenko, A. A. Zelensky, K. Egiazarian, and J. T. Astola, "Three-state locally adaptive texture preserving filter for radar and optical image processing," *EURASIP Journal on Applied Signal Processing*, vol. 2005, no. 8, pp. 1185–1204, 2005.

[17] N. N. Ponomarenko, V. V. Lukin, A. A. Zelensky, K. Egiazarian, and J. T. Astola, "Locally adaptive image filtering based on learning with clustering," in *Image Processing: Algorithms and Systems IV*, vol. 5672 of *Proceedings of SPIE*, pp. 94–105, San Jose, Calif, USA, January 2005.

[18] V. P. Melnik, V. V. Lukin, A. A. Zelensky, J. T. Astola, and P. Kuosmanen, "Local activity indicators for hard-switching adaptive filtering of images with mixed noise," *Optical Engineering*, vol. 40, no. 8, pp. 1441–1455, 2001.

[19] C. Oliver and S. Quegan, *Understanding Synthetic Aperture Radar Images*, SciTech, Raleigh, NC, USA, 2004.

[20] S. Solbo and T. Eltoft, "Homomorphic wavelet-based statistical despeckling of SAR images," *IEEE Transactions on Geoscience and Remote Sensing*, vol. 42, no. 4, pp. 711–721, 2004.

[21] V. V. Lukin, V. P. Melnik, V. I. Chemerovsky, S. Peltonen, and P. Kuosmanen, "Use of homomorphic transforms in locally adaptive filtering of radar images," in *Nonlinear Image Processing XI*, vol. 3961 of *Proceedings of SPIE*, pp. 184–195, San Jose, Calif, USA, January 2000.

[22] K. O. Egiazarian, V. P. Melnik, V. V. Lukin, and J. T. Astola, "Local transform-based denoising for radar image processing," in *Nonlinear Image Processing and Pattern Analysis XII*, vol. 4304 of *Proceedings of SPIE*, pp. 170–178, San Jose, Calif, USA, January 2001.

[23] J. S. Lee, "Refined filtering of noise using local statistics," *Computer Graphics and Image Processing*, no. 24, pp. 259–269, 1983.

[24] D. T. Kuan, A. A. Sawchuk, T. C. Strand, and P. Chavel, "Adaptive noise smoothing filter for images with signal-dependent noise," *IEEE Transactions on Pattern Analysis and Machine Intelligence*, vol. 7, no. 2, pp. 165–177, 1985.

[25] L. Klaine, B. Vozel, and K. Chehdi, "An integro-differential method for adaptive filtering of additive or multiplicative noise," in *Proceedings of IEEE International Conference on Acoustics, Speech and Signal Processing (ICASSP '05)*, vol. 2, pp. 1001–1004, Philadelphia, Pa, USA, March 2005.

[26] S. I. Sadhar and A. N. Rajagopalan, "Image estimation in film-grain noise," *IEEE Signal Processing Letters*, vol. 12, no. 3, pp. 238–241, 2005.

[27] L. Yaroslavsky and M. Eden, *Fundamentals of Digital Optics*, Birkhauser, Boston, Mass, USA, 1996.

[28] R. Coifman and D. L. Donoho, "Translation-invariant denoising," in *Wavelets and Statistics*, A. Antoniadis, Ed., vol. 103 of *Lecture Notes in Statistics*, pp. 125–150, Springer, New York, NY, USA, 1995.

[29] J. Portilla, V. Strela, M. J. Wainwright, and E. P. Simoncelli, "Image denoising using scale mixtures of Gaussians in the wavelet domain," *IEEE Transactions on Image Processing*, vol. 12, no. 11, pp. 1338–1351, 2003.

[30] D. L. Donoho and J. M. Johnstone, "Ideal spatial adaptation by wavelet shrinkage," *Biometrika*, vol. 81, no. 3, pp. 425–455, 1994.

[31] A. N. Akansu and R. A. Haddad, *Multiresolution Signal Decomposition: Transforms, Subbands, Wavelets*, Academic Press, San Diego, Calif, USA, 2nd edition, 2001.

[32] N. N. Ponomarenko, V. V. Lukin, K. Egiazarian, and J. Astola, "DCT based high quality image compression," in *Proceedings of the 14th Scandinavian Conference on Image Analysis (SCIA '05)*, vol. 3540 of *Lecture Notes in Computer Science*, pp. 1177–1185, Joensuu, Finland, June 2005.

[33] V. V. Lukin, N. N. Ponomarenko, L. Yu. Alekseyev, V. P. Melnik, and J. T. Astola, "Two-stage radar image despeckling based on local statistic Lee and sigma filtering," in *Nonlinear Image Processing and Pattern Analysis XII*, vol. 4304 of *Proceedings of SPIE*, pp. 106–117, San Jose, Calif, USA, January 2001.

[34] H. Huang, X. Lin, S. Rahardja, and R. Yu, "A method for realizing reversible integer type-IV discrete cosine transform (IntDCT-IV)," in *Proceedings of the 7th International Conference on Signal Processing (ICSP '04)*, vol. 1, pp. 101–104, Beijing, China, August-September 2004.

[35] O. G. Guleryuz, "Weighted overcomplete denoising," in *Proceedings of the 37th Conference Record of the Asilomar Conference on Signals, Systems and Computers*, vol. 2, pp. 1992–1996, Pacific Grove, Calif, USA, November 2003.

[36] K. Egiazarian, J. Astola, M. Helsingius, and P. Kuosmanen, "Adaptive denoising and lossy compression of images in transform domain," *Journal of Electronic Imaging*, vol. 8, no. 3, pp. 233–245, 1999.

[37] B. Aiazzi, S. Baronti, and L. Alparone, "Blind image estimation through fuzzy matching pursuits," in *Proceedings of IEEE International Conference on Image Processing (ICIP '01)*, vol. 1, pp. 241–244, Thessaloniki, Greece, October 2001.

[38] F. Argenti, G. Torricelli, and L. Alparone, "Signal-dependent noise removal in the undecimated wavelet domain," in *Proceedings of IEEE International Conference on Acoustics, Speech and Signal Processing (ICASSP '02)*, vol. 4, pp. 3293–3296, Orlando, Fla, USA, May 2002.

Ruşen Öktem was born in Turkey, in 1973. She received her B.S. degree in electrical and electronics engineering from Bilkent University, Turkey, in 1994, her M.S. and Ph.D. degrees in signal and image processing from Tampere University of Technology, Finland, in 1997 and 2000, respectively. She is working as an Assistant Professor at Electrical and Electronics Engineering Department of Atılım University, Ankara, Turkey, where she is teaching and leading or supporting state and EU projects. Her research topics include image enhancement, image compression, feature extraction, and stochastic processing of RF signals.

Karen Egiazarian was born in Yerevan, Armenia, in 1959. He received the M.S. degree in mathematics from Yerevan State University in 1981, the Ph.D. degree in physics and mathematics from Moscow State University, Moscow, Russia, in 1986, and the D.Tech. degree from Tampere University of Technology (TUT), Tampere, Finland, in 1994. He was a Senior Researcher with the Department of Digital Signal Processing, Institute of Information Problems and Automation, and National Academy of Sciences of Armenia. Since 1996, he has been an Assistant Professor with the Institute of Signal Processing, Tampere University of Technology, where he is currently a Professor, leading the Transforms and Spectral Methods Group. His research interests are in the areas of applied mathematics, signal processing, and digital logic.

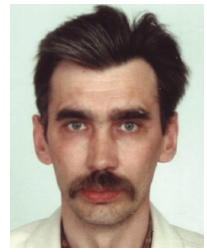

Vladimir V. Lukin graduated from Kharkov Aviation Institute (now National Aerospace University, Kharkov, Ukraine) and got diploma with honor in radioengineering. Since then, he has been with the Department of Transmitters, Receivers and Signal Processing of the same University. He received Candidate of Technical Science degree in 1988 and Doctor of Technical Science degree in 2002 and became Professor in 2003. He has published more than 250 journal and conference papers, more than 100 are in English. His research interests include remote sensing data processing, adaptive filtering of signals and images.

Nikolay N. Ponomarenko is a Senior Researcher of Department of Transmitters, Receivers and Signal Processing of National Aerospace University of Ukraine. He got a diploma in computer sciences from National Aerospace University of Ukraine in 1993, Candidate of Technical Sciences degree (in remote sensing area) from the Highest Attestation Commission of Ukraine in 2004, and Doctor of Technology degree (in image compression area) from Tampere University of Technology, Finland, in 2005. His research interests are image and video compression, denoising, and quality assessment.

Oleg V. Tsymbal graduated from National Aerospace University, Kharkov, Ukraine in 1998 and got diploma with honor in computer sciences. In 2003, he defended Candidate of Technical Science thesis in Ukraine, and in 2005, he got Doctor of Technology degree from Tampere University of Technology, Finland. Currently, he is with Visy Oy, Finland. His research interests include remote sensing data processing and adaptive image denoising.